https://ntrs.nasa.gov/search.jsp?R=19780025932 2020-03-22T01:47:07+00:00Z

General Disclaimer

One or more of the Following Statements may affect this Document

- This document has been reproduced from the best copy furnished by the organizational source. It is being released in the interest of making available as much information as possible.

- This document may contain data, which exceeds the sheet parameters. It was furnished in this condition by the organizational source and is the best copy available.

- This document may contain tone-on-tone or color graphs, charts and/or pictures, which have been reproduced in black and white.

- This document is paginated as submitted by the original source.

- Portions of this document are not fully legible due to the historical nature of some of the material. However, it is the best reproduction available from the original submission.

Produced by the NASA Center for Aerospace Information (CASI)

NASA Technical Memorandum 78785

IMPEDANCE MEASUREMENT USING
A TWO-MICROPHONE, RANDOM-EXCITATION METHOD

(NASA-TM-78785) IMPEDANCE MEASUREMENT USING A TWO-MICROPHONE, RANDOM-EXCITATION METHOD (NASA) 40 p HC A03/MF A01 CSCL 20A

N78-33875

Unclas
G3/71 33842

A. F. Seybert* and T. L. Parrott

October 1978

*Assistant Professor at the University of Kentucky

National Aeronautics and
Space Administration

Langley Research Center
Hampton, Virginia 23665

SUMMARY

A study is conducted to determine the feasibility of using a two-microphone, random-excitation technique for the measurement of acoustic impedance. Equations are developed, including the effect of mean flow, which show that acoustic impedance is related to the pressure ratio and phase difference between two points in a duct carrying plane waves only. Tests are conducted to determine the feasibility of this approach. The impedance of a honeycomb ceramic specimen and a Helmholtz resonator are measured and compared with the impedance of these specimens obtained using the conventional standing-wave method. Agreement between the two methods is generally good but some systematic differences exist. A sensitivity analysis is performed to pinpoint possible error sources and recommendations are made for future study. The two-microphone approach evaluated in this study appears to have some advantages over other impedance measuring techniques. Possible advantages include: application to problems where flow noise is dominant, better resolution of experimental data and significant reduction of time required for testing with potential for near real time impedance measurements.

INTRODUCTION

An accurate knowledge of acoustic impedance is important for optimizing noise attenuation of acoustic absorbers for turbomachinery ducts. Because most practical absorbers used for duct treatments do not lend themselves to mathematical modeling, acoustic impedance must be measured. The objective of this study was to test the feasibility of a new impedance measuring technique by comparing the results with those obtained using the conventional standing wave method. A narrow band and broadband absorber were used as test specimens.

In the last several years a number of new impedance measuring methods have been proposed. Those based on stationary microphone systems will be briefly reviewed. Gately and Cohen[1]* used a gated sine wave to determine the impedance of small acoustic filters used with refrigeration compressors. By using a long tube upstream of the acoustic filters, they were able to separate the incident and reflected sound waves. This experimental arrangement allowed them to measure the incident and reflected wave amplitudes, as well as the phase shift between the waves. Schmidt and Johnston[2] used a pair of closely spaced microphones to measure the reflection coefficient of orifices. However, they had problems in determining phase angle and therefore did not measure acoustic impedance. Melling[3] used a "two-microphone" method to measure the acoustic impedance of perforates. Singh and Katra[4] used a pulse technique to measure the reflection coefficient of small acoustic filters. Like Gately and Cohen, they used a long tube to separate the incident and reflected waves.

*Numbers in brackets refer to list of cited references at the end of this report.

Long tube lengths needed for techniques proposed by Gately and Cohen[1] and Singh and Katra[4] may result in unwanted dissipation. On the other hand, discrete frequency techniques, such as used by Schmidt and Johnston, are time consuming, and may not be well suited for practical acoustical testing.

Seybert and Ross[5] used a two-microphone, random-excitation technique to study acoustic impedance of automotive mufflers. They showed that for a plane wave sound field, the incident and reflected waves could be separated by measuring the cross-spectrum between two microphones located at fixed positions in the duct. Thus, in addition to measuring acoustic impedance, this method can also determine the incident and reflected sound power in a duct. Recently, Blaser and Chung[6] have used this method to evaluate internal combustion engine exhaust systems.

The remainder of this report discusses the application of the two-microphone technique of Seybert and Ross to measurement problems in duct acoustics. This work was carried out during a ten-week period during which the first author was supported by a fellowship provided by NASA and the American Society for Engineering Education.

...

SYMBOLS

A	amplitude of incident wave, dynes/cm^2
$\tilde{B}$	complex amplitude of reflected wave, dynes/cm^2
c	sound speed, cm/sec
f	frequency, Hz
i	imaginary unit
K	free space wave number, cm^{-1}
K_i	incident wave number, cm^{-1}
K_r	reflected wave number, cm^{-1}
M	flow mach number
$\tilde{P}_i$	incident acoustic pressure dynes/cm^2
$\tilde{P}_r$	reflected acoustic pressure (complex) dynes/cm^2
$\tilde{P}_{12}$	pressure ratio between X_1 and X_2
$\tilde{R}$	reflection factor (complex)
R	reflection coefficient
v	flow velocity, cm/sec
X	axial coordinate, cm
X_1, X_2	microphone positions, cm
$\tilde{Z}$	acoustic impedance, normalized by ρc
$\tilde{Z}_m$	measured axial impedance, normalized by ρc
$\tilde{Z}_r$	resonator impedance, normalized by ρc
$\tilde{Z}_t$	termination impedance, normalized by ρc
ω	angular frequency, $2\pi f$
ϕ	angle between P_i and P_r, radians
θ	acoustic resistance, normalized by ρc
X	acoustic reactance, normalized by ρc
ρ	density of air, gm/cm^3

THEORETICAL CONSIDERATIONS

Figure 1 is a diagram showing a rigid tube containing an acoustic medium that is excited by a vibrating piston or other acoustic source. The tube is terminated at the coordinate origin by an acoustic system with unknown acoustic impedance Z(f). Assuming only a plane-wave sound field in the tube, the incident and re lected sound pressure waves can be expressed by:

$$\tilde{P}_i(x_1 t) = Ae^{i(wt-K_i x)} \tag{1}$$

$$\tilde{P}_r(x_1 t) = \tilde{B}\, e^{i(wt + K_r x)} \tag{2}$$

where

$$K_i = \frac{K}{1 + M}\ ,\ K_r = \frac{K}{1 - M},\ K = \frac{w}{c},\ M = \frac{v}{c}$$

and where v is the mean flow speed and c is the speed of sound.

The total acoustic pressure at any point in the tube is the sum of the incident and reflected pressure waves. The ratio of the sound pressure between two points x_1 and x_2 is:

$$\frac{\tilde{P}_1}{\tilde{P}_2} = \tilde{P}_{12} = P_{12}e^{i\phi_{12}} = \frac{Ae^{-iK_i x_1} + \tilde{B}e^{iK_r x_1}}{Ae^{-iK_i x_2} + \tilde{B}e^{iK_r x_2}} \tag{3}$$

The complex reflection coefficient $\tilde{R}$ at x = 0 is defined

$$\tilde{R} = Re^{i\phi} = \frac{\tilde{B}}{A} \tag{4}$$

and $\tilde{R}$ is related to the impedance $\tilde{Z}(f)$ by

$$R = \frac{\tilde{Z}(f) - 1}{\tilde{Z}(f) + 1} \tag{5}$$

Combining equations 1 through 5 and solving for $\tilde{Z}(f)$ yields;

$$\tilde{Z}(f) = \frac{(e^{-iK_i x_1} - e^{iK_r x_1}) - \tilde{P}_{12}\,(e^{-iK_i x_2} - e^{ik_r x_2})}{\tilde{P}_{12}(e^{-iK_i x_2} + e^{iK_r x_2}) - (e^{-iK_i x_1} + e^{-iK_i x_1})} \tag{6}$$

Equation 6 gives a potentially useful way to calculate the acoustic impedance from measured values of pressure ratio P_{12} and phase angle ϕ_{12} between two points in a one-dimensional acoustic field.

Although equation 6 was derived assuming a harmonic sound pressure field, reference 5 generalizes the technique to include a random sound field.

EXPERIMENTAL SETUP

A series of tests was conducted to determine the feasibility of using equation 6 to calculate acoustic impedance. Two acoustic systems

were used for the evaluation: a Helmholtz resonator with a resonant frequency of approximately 1.0 kHz and a sample of a ceramic honeycomb material. To evaluate the two-microphone method (TMM), a comparison was made with impedance data obtained using the standing-wave method[8] (SWM). For the TMM both pure tone and broad-band random excitation were used but the SWM data were based on pure-tone excitation. Tests without flow were conducted with the resonator in a normal and grazing incidence orientation, but the ceramic specimen was evaluated only in a normal incidence orientation (in a grazing incidence orientation the area of the ceramic specimen was sufficiently large to violate the assumption of a lumped parameter system). A final set of tests was conducted with the Helmholtz resonator in the presence of a mean flow with Mach numbers of 0.025 and 0.10.

Figure 2 shows a schematic of the instrumentation used for the TMM tests. Figures 2a and 2b shows the instrumentation used with the pure-tone and broad band random excitation respectively. For all the tests the microphones were mounted flush in the tube wall and were separated by a distance of 2.54 cm (1.00 in.). In the no-flow impedance tube (used for the normal incidence tests) the microphones were located at distances of 21.24 cm (8.36 in.) and 23.78 cm (9.36 in.) from the end of the tube where the test specimen was located. In the flow impedance tube the microphones were located 53.34 cm (21.00 in.) and 55.88 cm (22.00 in.) from the specimen (in the flow impedance tube the specimen is a side-branch system in parallel with the tube termination impedance).

TEST RESULTS

Figures 3a and 3b show the resistance and reactance (normalized by ρc) of the ceramic specimen in the no-flow tube as determined from both the SWM and the TMM. Both pure-tone excitation (6-21-78) and broad-band random excitation (6-27-78) were used with the TMM. In general, there is good agreement between the results of the TMM and the SWM. A discussion of the detailed differences between the results will be presented later in this report.

Figure 4 shows the measured pressure ratio and phase angle (i.e., complex pressure ratio between mics 1 and 2) used to calculate the acoustic impedance of the ceramic specimen for broad-band excitation. The details of these curves depend not only on the resonator properties but also on the geometry of the experimental setup (i.e., x_1, x_2 and $(x_2 - x_1)$. For example the frequencies where $|P_{12}| = 1(0\ dB)$ and where ϕ_{12} is maximum indicate that a null in the standing wave pattern lies between the two microphone positions. Also the onset of higher order modes can be observed near 3500 Hz.

Figure 5 shows the auto-spectra of the two microphones for the test case using the ceramic specimen excited by broad-band random noise. These spectra are similar but are different in detail. The small scale fluctuations in the spectra result from the changing standing wave structure as frequency changes.

Figure 6 shows the sound pressure auto-spectrum (Lp) measured by a probe tube near the face of the ceramic sample and the spectrum of the

input voltage (L_v) to the acoustic driver. Tests confirmed (fig. 4) that the impedance of the ceramic specimen was linear over a range of sound pressure level at the specimen face from 90 to 110 dB; therefore it was not necessary for the sound pressure spectrum at the face of the specimen to be flat. On the other hand, a flat spectrum is required when testing a specimen with a non-linear impedance. This topic will be discussed in further detail at another location in this report.

Helmholtz Resonator

A second test was conducted in which the test specimen was a Helmholtz resonator. The resonator had a cylindrical cavity 5.08 cm (2.00 in.) long and 3.81 cm (1.50 in.) in diameter. The resonator opening (oriented perpendicular to the impedance tube axis) was a slit parallel to the axis of the cylinder, 5.08 cm (2.00 in.) long and 0.25 cm (0.10 in.) wide. The thickness of the resonator neck was 0.0127 cm (0.0050 in.). The resonator was tested in a normal incidence orientation and a grazing incidence orientation (no flow) using both the TMM and the SWM. For the grazing incidence tests the resonator impedance was computed assuming the resonator was a lumped impedance, $\tilde{Z}_r$, in parallel with the tube termination impedance, $\tilde{Z}_t$:

$$\frac{1}{\tilde{Z}_m} = \frac{1}{\tilde{Z}_r} + \frac{1}{\tilde{Z}_t} \tag{7}$$

Therefore the measurement of $\tilde{Z}_m$ and $\tilde{Z}_t$ permit $\tilde{Z}_r$ to be calculated. In this experiment $\tilde{Z}_t$ was estimated to be 1 corresponding to a non-reflective termination.

Figure 7 shows data comparing the resonator impedance using both the TMM and SWM. The reactance data shows good agreement between the two techniques; each technique reveals a shift in the resonance frequency of the resonator.* The cause of the large discrepancy between the resistance data in the grazing incidence test is not clear. Pure tone SWM tests indicated however that the resonator was highly nonlinear above 90 dB SPL at the slit. For random excitation the spectrum level was adjusted to 90 dB at the resonator resonance frequency but exceeded 90 dB at other frequencies which may have been a contributing factor in the large discrepancy.

Tests with Flow

Figure 8 shows the reactance of the Helmholtz resonator for Mach numbers of 0.0, 0.025, and 0.10 as measured by the TMM. This data is qualitatively consistent with acoustic theory and other experimental data showing that grazing flow decreases the mass reactance of a resonator, thereby increasing the resonant, frequency.

DISCUSSION OF RESULTS

In general, the agreement between the TMM and the SWM is good. On the other hand, some detailed discrepancies do exist. It was found, for

*This shift in resonance is believed to be due to a change in the radiation impedance of the resonator. Ingard[7] has studied the radiation loading on resonators in a normal incidence orientation, but there is no similar study for grazing incidence.

example, that difficulty in accurately measuring phase angle using the experimental setup in figure 2a resulted in some scatter of the data, (note the resistance data in figure 7 for the TMM pure-tone excitation). An error analysis of equation 6 showed that the accuracy of the resistance is strongly influenced by accurate phase measurements. The repeatibility and accuracy of phase measurements using the SD360 (fig. 2b) is better than that obtained using the analog phase meter. As might be expected, phase angle accuracy is very important when the true phase angle approaches 0 or π.

Figures 9 through 13 show the results of a sensitivity study using the ceramic specimen data (figs. 3a and 3b). Figures 9a and 9b show the sensitivity of the impedance to small errors in phase angle measurement ($\pm 2°$). The largest effect is noted in the resistance at low frequencies (500 - 700 Hz) where the phase angle is small (see fig. 4). An error in phase angle measurement also seems to affect the reactance at frequencies where the absolute value of the reactance is large (see fig. 9b).

Figures 10a and 10b show the effect on impedance of small variations in the level of the measured pressure ratio ($\pm$ 0.1 dB). An accuracy within 0.1 dB is achievable using standard laboratory sound measuring equipment because the absolute accuracy of the sound pressure is not important. One microphone was amplitude and phase calibrated relative to the other by flush mounting in a smooth rigid piston which was installed in the standing wave tube so that plane waves were normally

incident on the surface. The microphones were symmetrically located with respect to the piston axis. Therefore, it was assumed that both microphones would experience phase coherent pressure fluctuations. These calibration data were used to correct the measured phase angles and pressure ratios for each specimen].

Figures 11a and 11b show the variation of impedance with temperature in the tube. A higher temperature appears to shift the resistance toward lower frequencies. A higher temperature affects the reactance by decreasing its value near the anti-resonance frequency (2000 Hz).

The discrepancies noted in figures 3a and 3b are probably due to, in part, an inaccurate knowledge of the true temperature in the tube when the measurements were made. When these tests were made the temperature in the tube was assumed to be the same as the room temperature. Later, this assumption was found to be false, and in subsequent tests the tube temperature was measured.

Figures 12 and 12b show the effect of slight errors in the absolute position of the microphone, while figures 13a and 13b show the effect of small variations in the microphone spacing. The microphone locations can be determined to an accuracy of less than 0.1 cm using the microphone positioning system of the impedance tube, and the microphone spacing can be controlled to within 0.01 cm. However, the data in figure 13a and 13b raise the question: Is the acoustical spacing between the microphones equal to the distance between the microphone centerlines? If these distances are different, using the centerline distance will generate errors in calculating the impedance.

Grazing incidence tests. - For the grazing incidence tests the specimen was assumed to be a side branch in parallel with the tube termination, and the specimen impedance, $\tilde{Z}_r$, was calculated using equation 7 assuming $\tilde{Z}_t = 1$. However, when the specimen resistance is quite small and/or the specimen reactance is large any deviation of $\tilde{Z}_t$ from the assumed value of 1 may cause errors in calculating the specimen impedance. Some of the scatter in the data in figures 7 and 8 may be due to this effect.

Broad-band random excitation is well suited for acoustic testing because the data can be processed rapidly (if the appropriate hardware is available) and because the data is a continuous, rather than discrete, function of frequency. However, some problems associated with random excitation are revealed in the tests conducted as a part of this study. A uniform spectral density at the face of a specimen could not be generated with available equipment during this study. As suggested previously, a uniform spectral density might have produced better agreement with the pure tone SWM resistance because of nonlinear properties at the resonator above 90 dB. It is not clear why the computed resistance is a minimum near 1000 Hz (the resonator resonance) and is maximum near 500 and 1200 Hz for the case where random excitation was used. A sound pressure measurement at the face of the specimen revealed that the sound pressure spectrum had similar characteristics. However, the resonator nonlinearity is sensitive to particle velocity which is relatively large at the resonant frequency.

The problem of a non-uniform spectral density also affects the computation of the specimen reactance (see fig. 7) when the specimen is a

side branch. This is because the specimen reactance is a function of the measured impedance $\tilde{Z}_m$ (both reactance and resistance), see equation 7.

In processing broad-band random data there are a number of considerations that should be addressed. Some of these include: the effect of bandwidth, data window, and averaging procedure on bias and random errors; the statistical stability of the equations; and the effect of flow noise on the data analysis.

The effect of the frequency bandwidth used in the data analysis can be seen by plotting the standing wave for several different bandwidths. Figure 14 shows some of this data for the Helmholtz resonator in a grazing incidence location in the flow impedance tube. It can be seen that, for broad-band excitation, the standing wave ratio decreases as bandwidth and distance from the specimen increase.

Flow noise will be a problem for any measurement technique unless special data processing operations are performed to enhance the acoustic signal. (Some of the data variation in figure 8 is, no doubt, due to flow noise effects). One method for removing flow noise involves the measurement of the signal coherence between the driver input voltage and a microphone in the tube. When the microphone spectrum (flow noise plus sound) is multiplied by the signal coherence, the result is the spectrum of the acoustical signal. This is illustrated in figure 15 where the top curve is the sound pressure spectrum with a Mach number 0.3. The two lower curves are (1) the true acoustic spectrum (no flow) and (2) the acoustic spectrum obtained by the coherence procedure. Except for very low frequencies where background noise is present, it can be seen that

the no flow and flow acoustic spectra are the same (note that in some cases the acoustic spectrum is as much as 15 dB below the total spectrum).

CONCLUSIONS AND RECOMMENDATIONS

Based on the tests conducted during this study the two-microphone method appears to be a useful technique for evaluating acoustic impedance. It should be noted that this research effort was only a feasibility study, and that the two-microphone method is in a preliminary stage of development. Continued development and application of the two-microphone technique is recommended for the following reasons:

1. There is a need for additional ways to measure acoustic impedance, particularly in situations where it is necessary to confirm impedance data by two or more measurement methods.
2. There are some cases where the two microphone method may have an advantage over other impedance measuring techniques. The two microphone method has the potential to be extended to more difficult impedance measuring situations such as the measurement of impedance at low intensity and high Mach numbers using a signal coherence approach to enhance the acoustic signal.
3. Measurement time is reduced by at least an order of magnitude by using the two-microphone method with broad-band random excitation. The technique lends itself easily to automation using an on-line computer to process the data.
4. The two microphone method is a unique way of examining the wave structure of an acoustic field. This approach could be exploited

to develop other ideas related to duct acoustics, such as the separation of incident and reflected sound power in an acoustic field.

The two-microphone method is still under development and a number of items should be addressed to improve the reliability of the technique. Some suggested topics of study are:

1. Optimization of the two-microphone method. - A study of this type would determine the best location of the microphones and the optimum microphone spacing. The study would also determine the importance of microphone size on bias error in measuring the pressure ratio and phase shift between the microphones.
2. Error Analysis of the two-microphone method. - This would be composed of two parts: an error analysis of the impedance relation (eq. 6) in which all the relevant experimental parameters would be examined, and a statistical study to determine the effect on impedance calculations of data processing parameters such as bandwidth and data window. The result of this study would be the development of error bounds and confidence levels to establish the validity of impedance data.
3. Extension of two-microphone method to handle flow noise contamination. - This effort would involve modifying the signal processing procedures to utilize signal coherence techniques to enhance an acoustic signal buried in flow noise. Such a procedure would be useful for measuring the impedance of nonlinear systems at low and medium intensities when flow noise is present.

ORIGINAL PAGE IS
OF POOR QUALITY

4. Testing of non-linear systems with random excitation. - The problem of the inability to produce a flat spectrum at the face of the specimen can be handled in two ways. One method is to generate the random signal digitally, using digital filtering techniques to shape the spectrum of the driver voltage to yield a flat spectrum at the face of the specimen. A second method ignores the shape of the spectrum entirely but the spectrum level for each frequency band is recorded and stored in computer memory at the time the test is conducted. This procedure is repeated for several tests at different intensity levels, generating a three dimensional array (impedance, frequency, intensity). To determine the impedance at a certain intensity the array would be scanned at each frequency to find the appropriate impedance corresponding to the specified intensity (in certain cases interpolation may be necessary).

REFERENCES

1. Gately, W. S. and Cohen, R.: Methods for Evaluating the Performance of Small Acoustic Filters. J. Acoust. Soc. Am. 46, 6-16, 1969.

2. Schmidt, W. E. and Johnston, J. P.: Measurement of Acoustic Reflection from Obstructions in a Pipe with Flow. NSF Report PD-20, March 1975.

3. Melling, T. H.: The Acoustic Impedance of Perforates at Medium and High Sound Pressure Levels. J. Sound Vib. 20, 1-66, 1973.

4. Singh, R. and Katra, T.: On the Dynamic Analysis and Evaluation of Compressor Mufflers. Proceedings 1976 Purdue Compressor Technology Conference, July 6-9, 1976, (Purdue University, West Lafayette, IN, 1976).

5. Seybert, A. F. and Ross, D. F.: Experimental Determination of Acoustic Properties Using a Two-Microphone, Random-Excitation Technique. J. Acoust. Soc. Am. Vol. 61, No. 5, May 1977, pp. 1362-1370.

6. Blaser, D. A. and Chung, J. Y.: A Transfer Function Technique for Determining the Acoustic Characteristics of Duct Systems with Flow. Proceedings Inter Noise 78, San Francisco, CA, May 8-10, 1978, pp. 901-908.

7. Ingard, Uno: On the Theory and Design of Acoustic Resonators. J. Acoust. Soc. Am., vol. 25, no. 6, 1037-1061, 1953.

8. Impedance and Absorption of Acoustical Materials by the Tube Method. ASTM designation: C384-58 (Reapproved 1972). Part 18 of 1975 Annual Book of ASTM Standards, c. 1975, pp. 115-126.

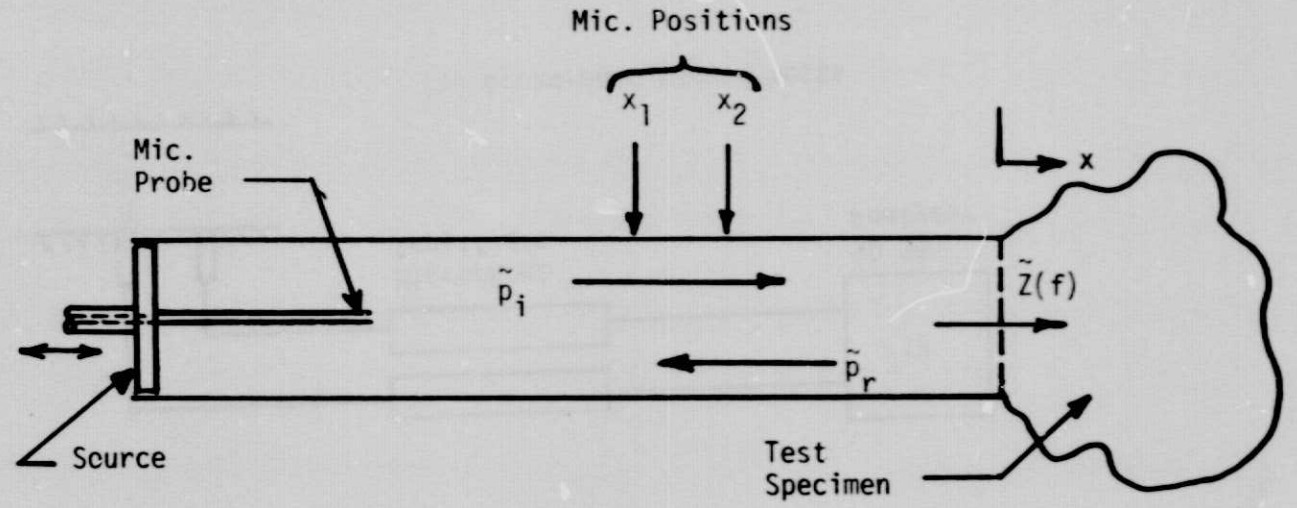

Figure 1.- Schematic diagram of experimental setup for comparing measurements of normal incidence impedance using both standing wave method (SWM) and two-microphone method (TMM).

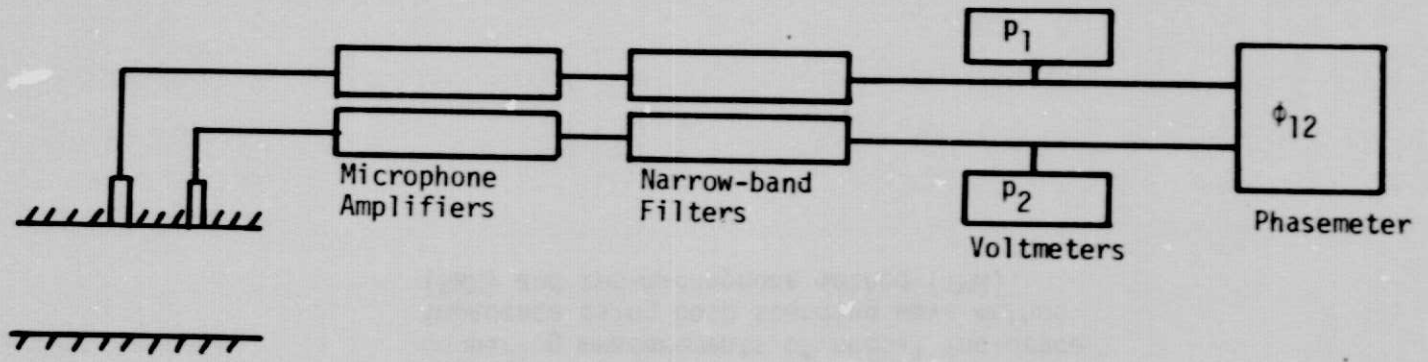

(a) Pure tone tests

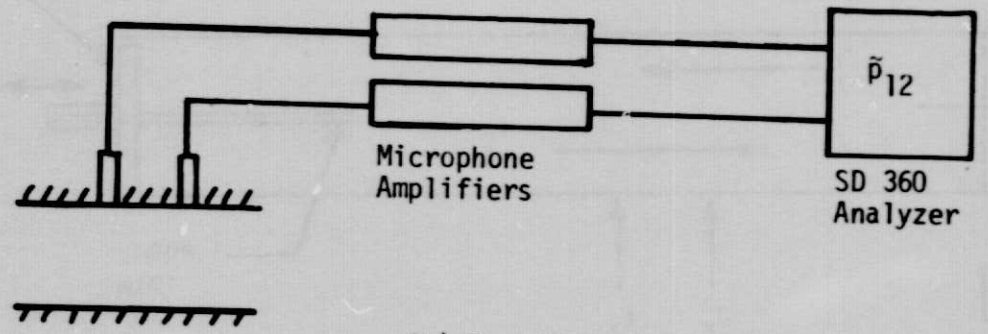

(b) Broad-band random tests

Figure 2. - Instrumentation for two-microphone method.

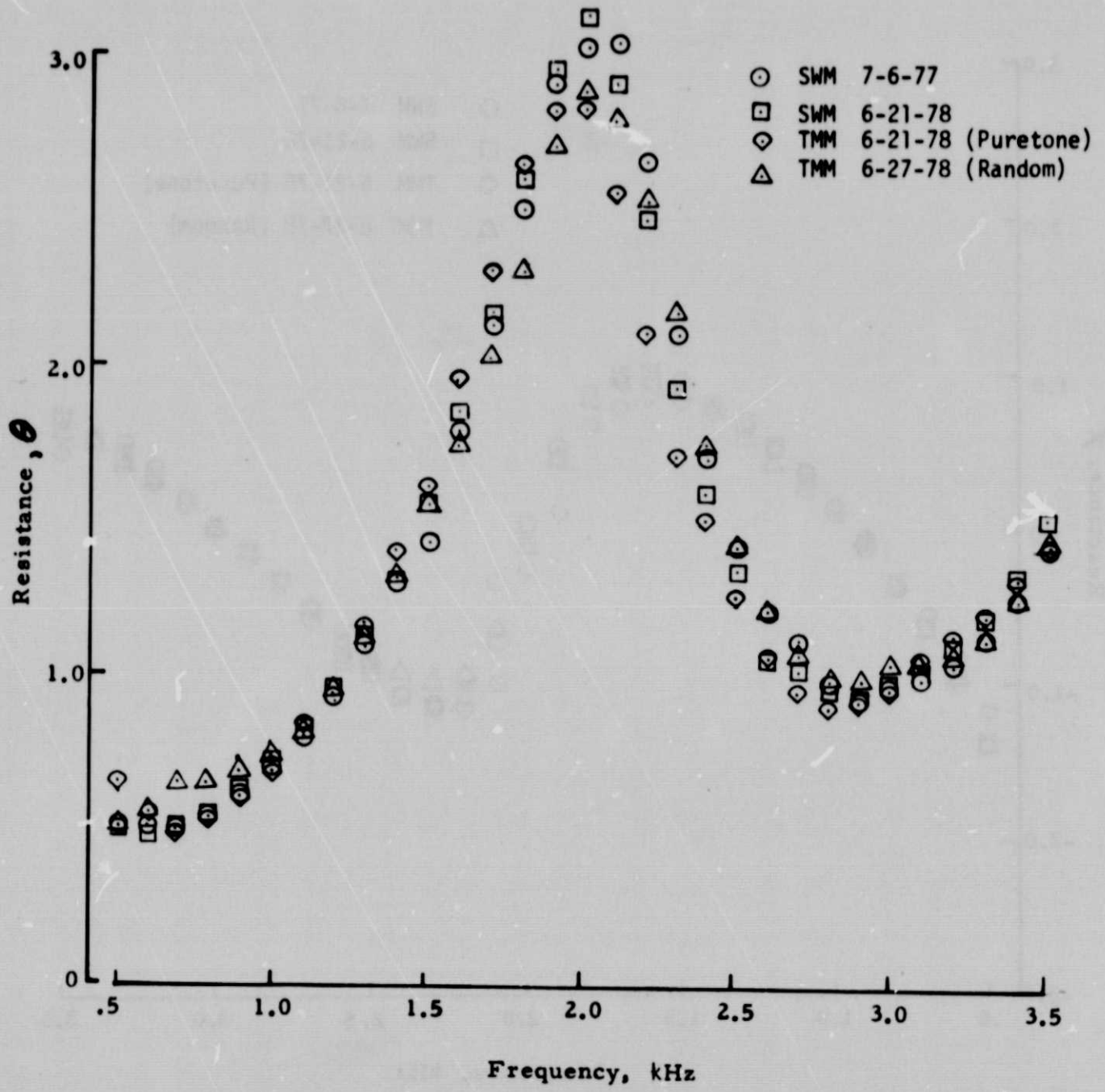

Figure 3a. - Resistance of the honeycomb ceramic specimen.

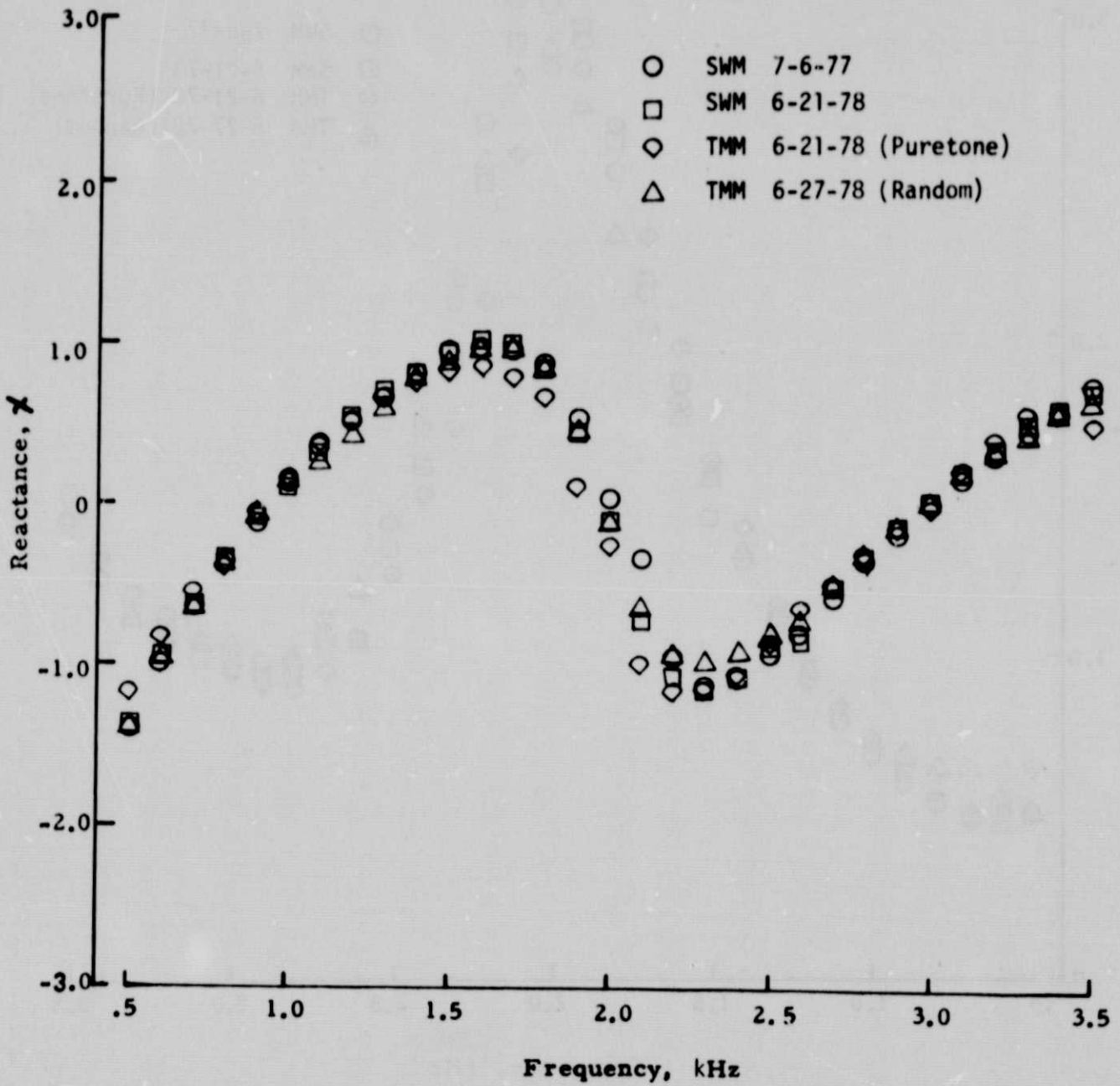

Figure 3b. - Reactance of the honeycomb ceramic specimen.

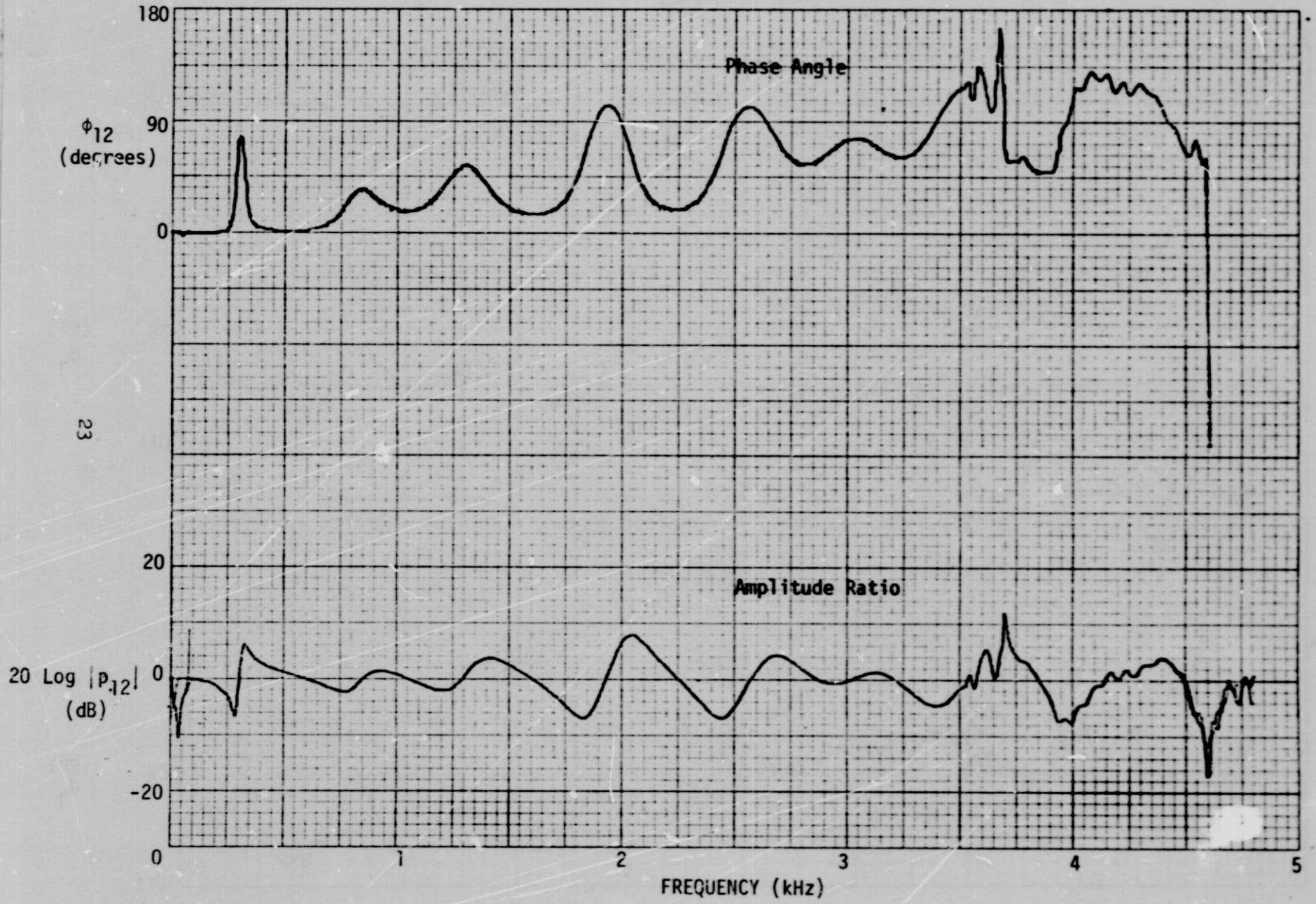

Figure 4.- Complex pressure ratio (phase angle and amplitude ratio) between microphone signals for ceramic specimen in no-flow impedance tube-overlay of data at 90 dB and 110 dB (2000 Hz, measured at sample face).

ORIGINAL PAGE IS
OF POOR QUALITY

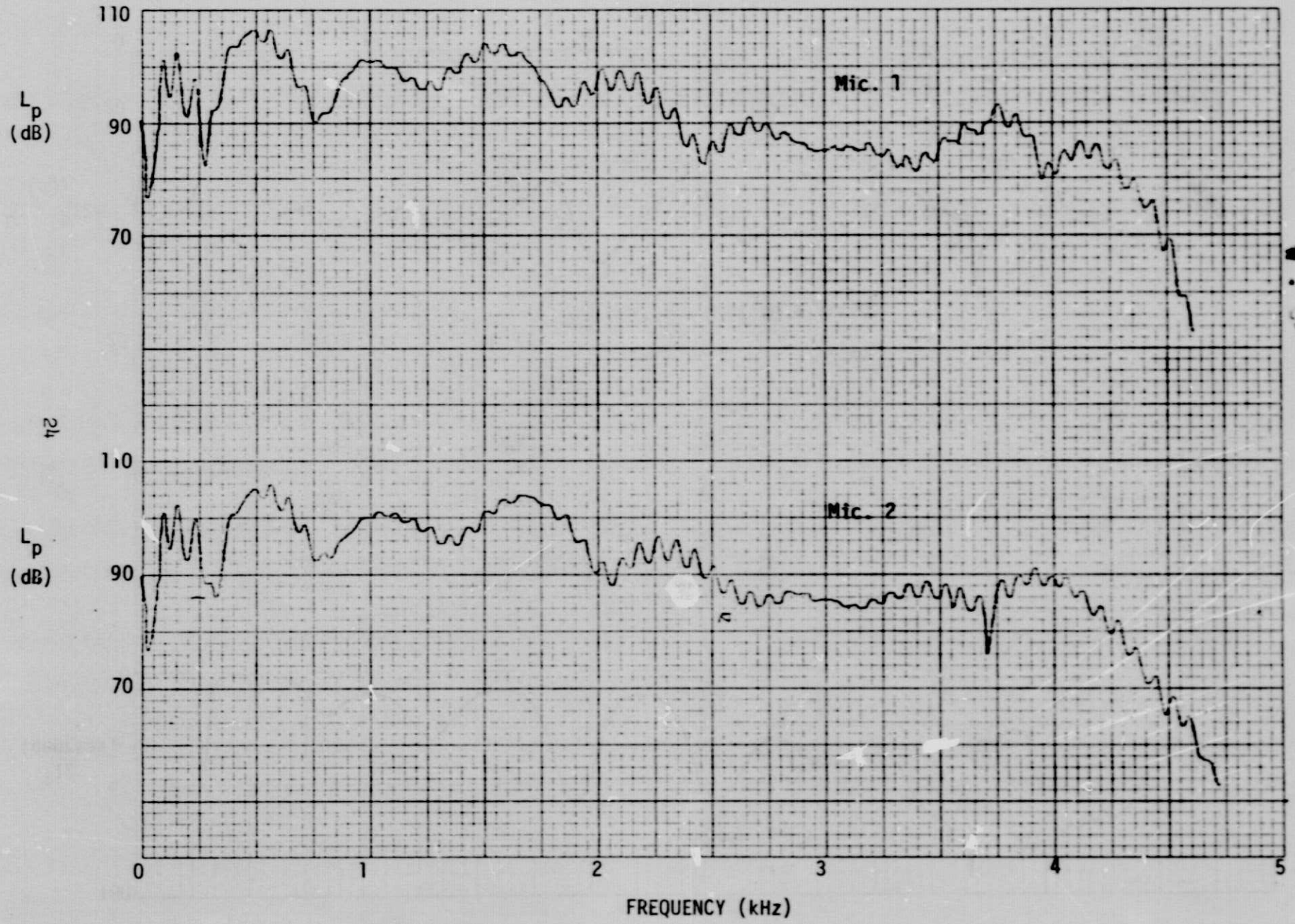

Figure 5. - Microphone spectra (Δf = 10 Hz) - microphone #1 (top); microphone #2 (bottom).

ORIGINAL PAGE IS OF POOR QUALITY

Figure 6. - Spectrum of sound pressure at face of sample (top) and spectrum of driver voltage (bottom).

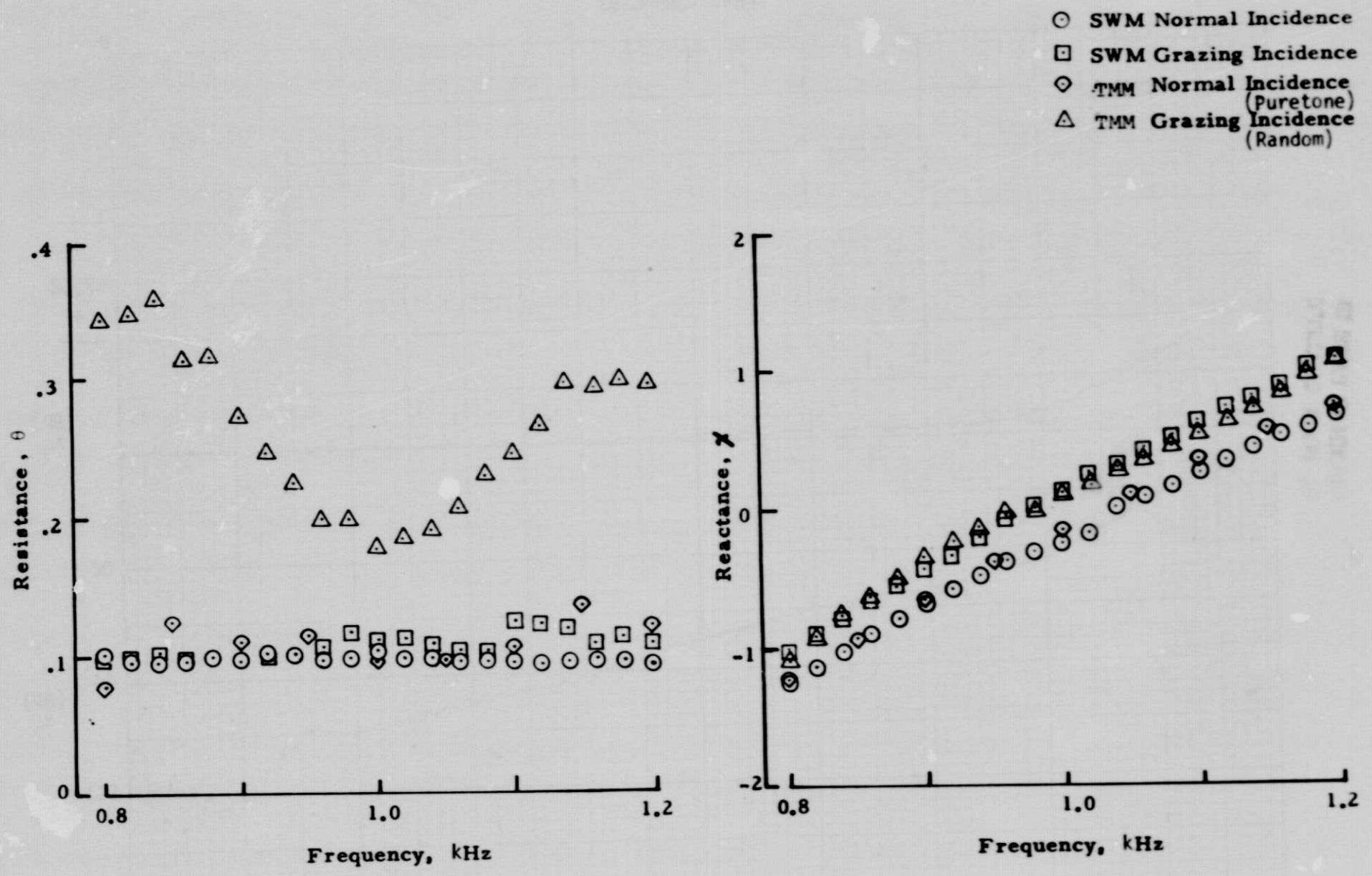

Figure 7. - Comparison of impedance data for a Helmholtz resonator using the two-microphone method (TMM) and the standing wave method (SWM).

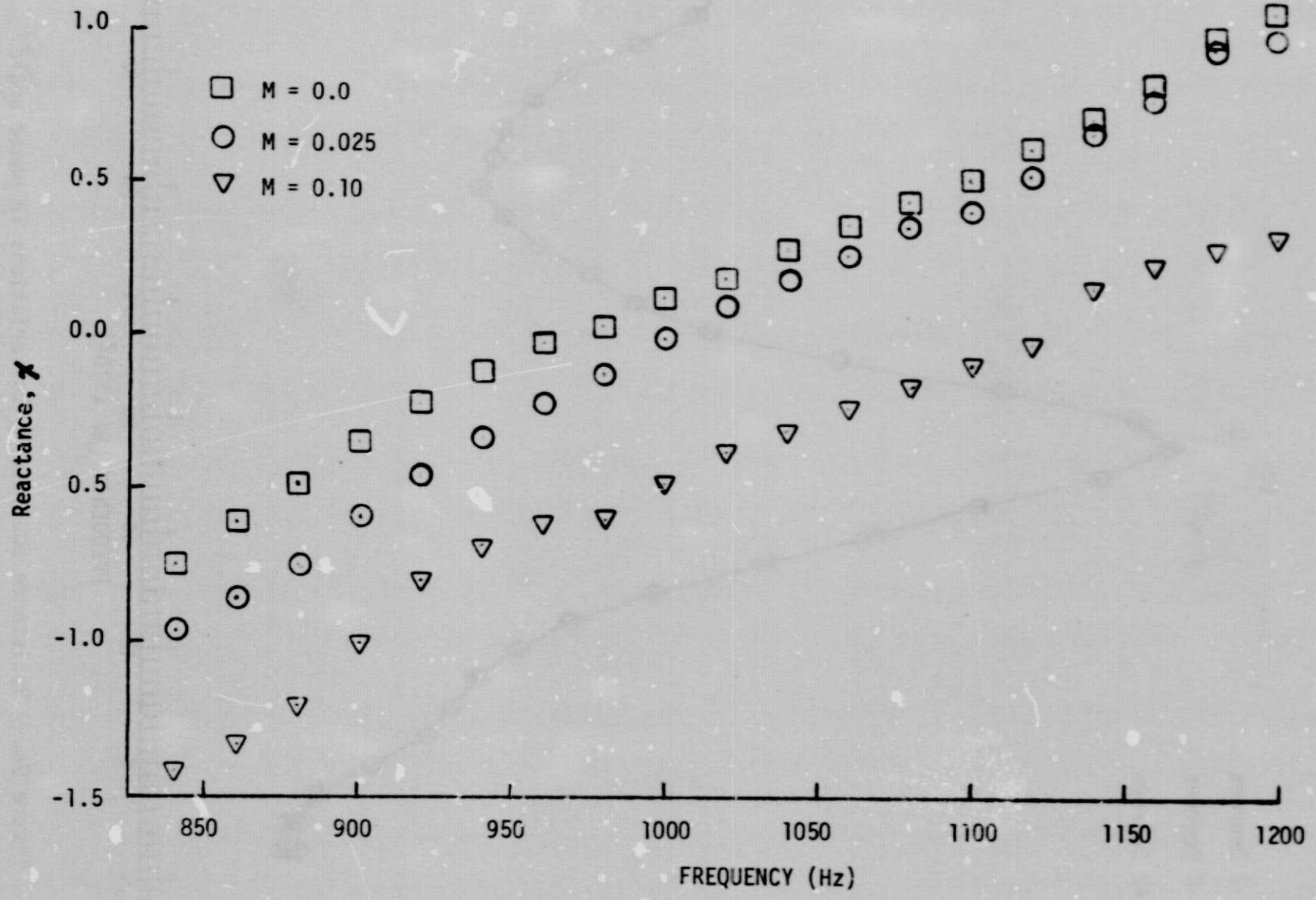

Figure 8. - The effect of grazing flow on the reactance of a slit Helmholtz resonator.

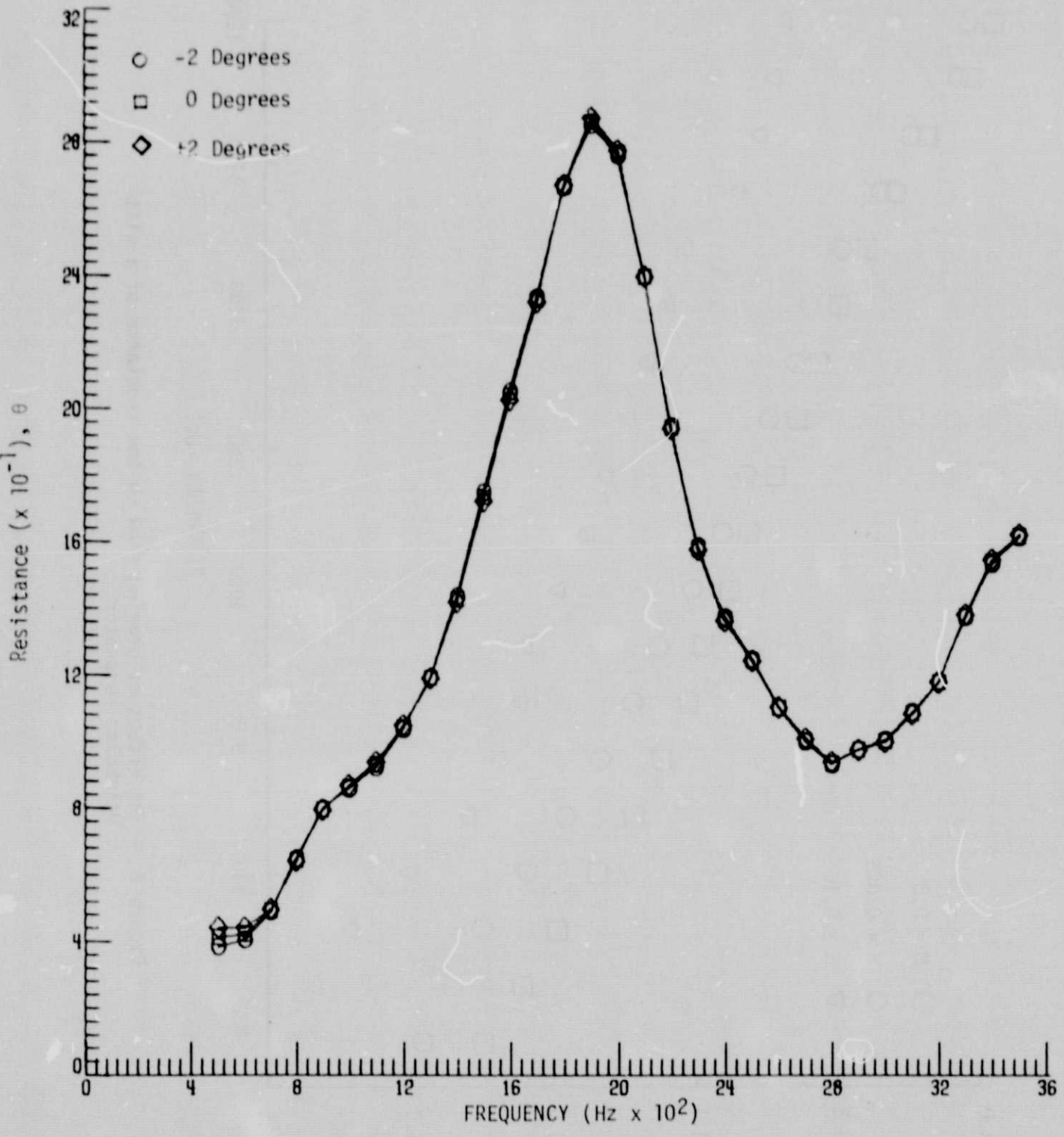

Figure 9a. - Resistance sensitivity to variations in phase angle.

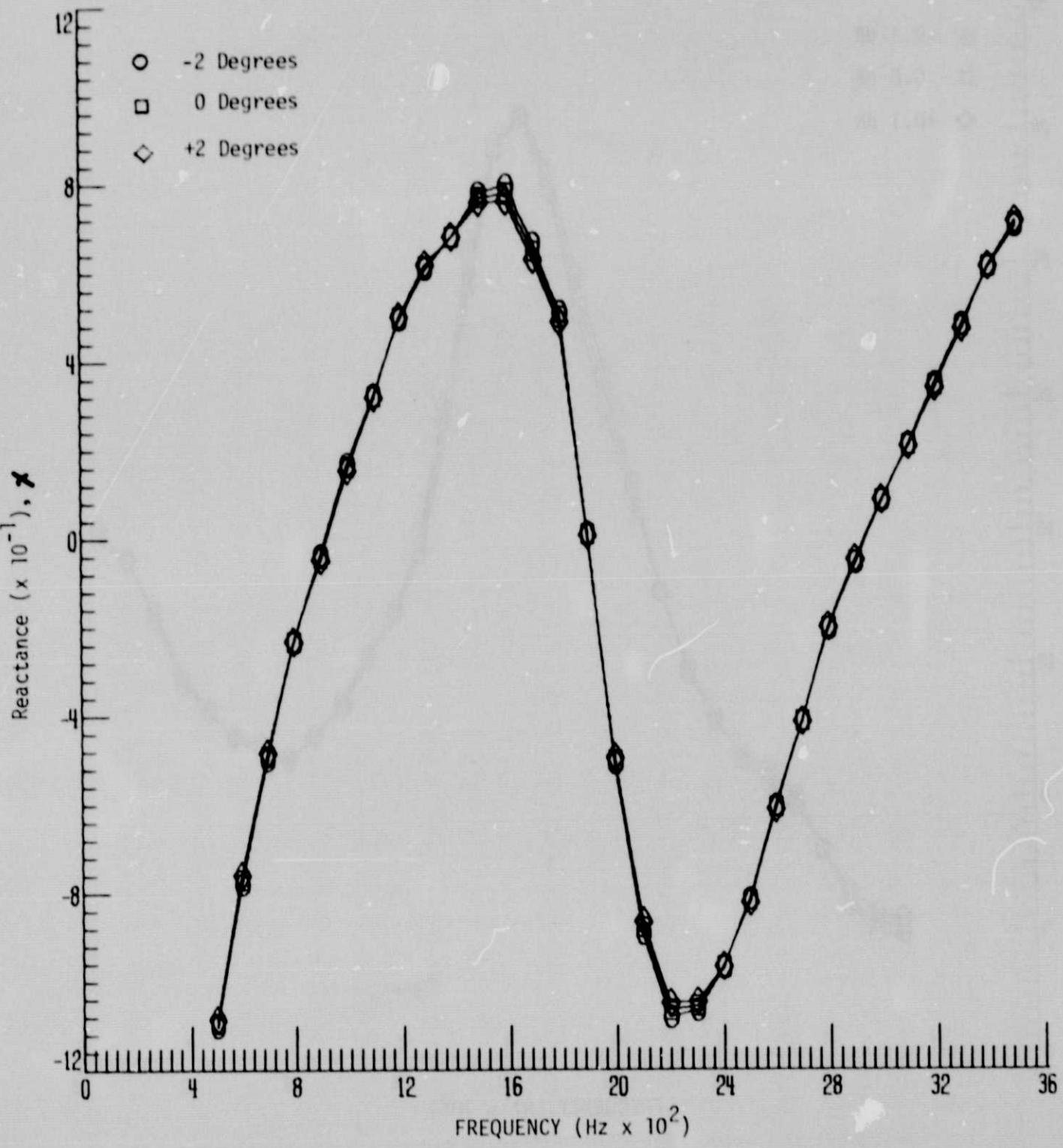

Figure 9b. - Reactive sensitivity to variations in phase angle.

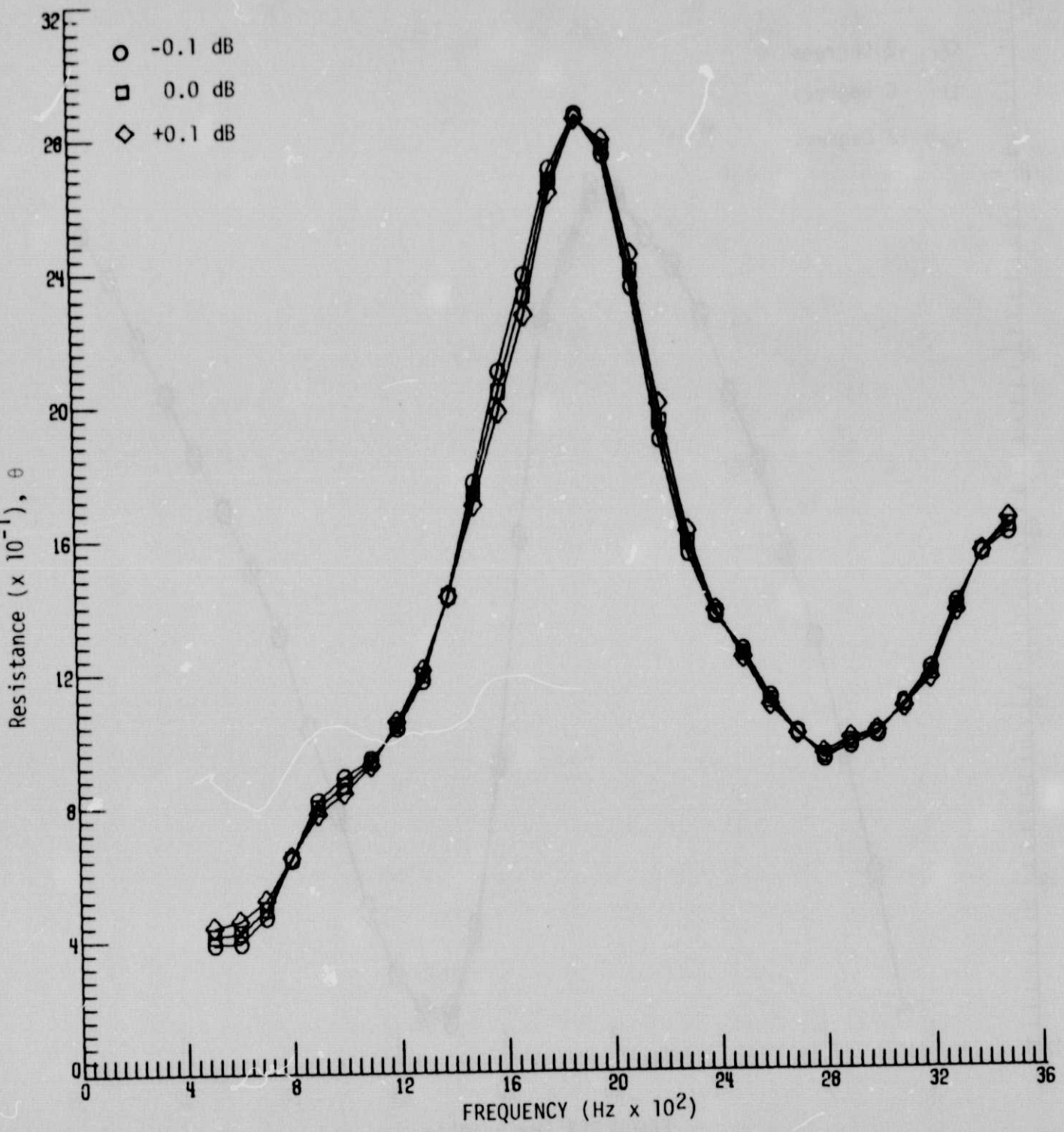

Figure 10a. - Resistance sensitivity to variations in pressure ratio.

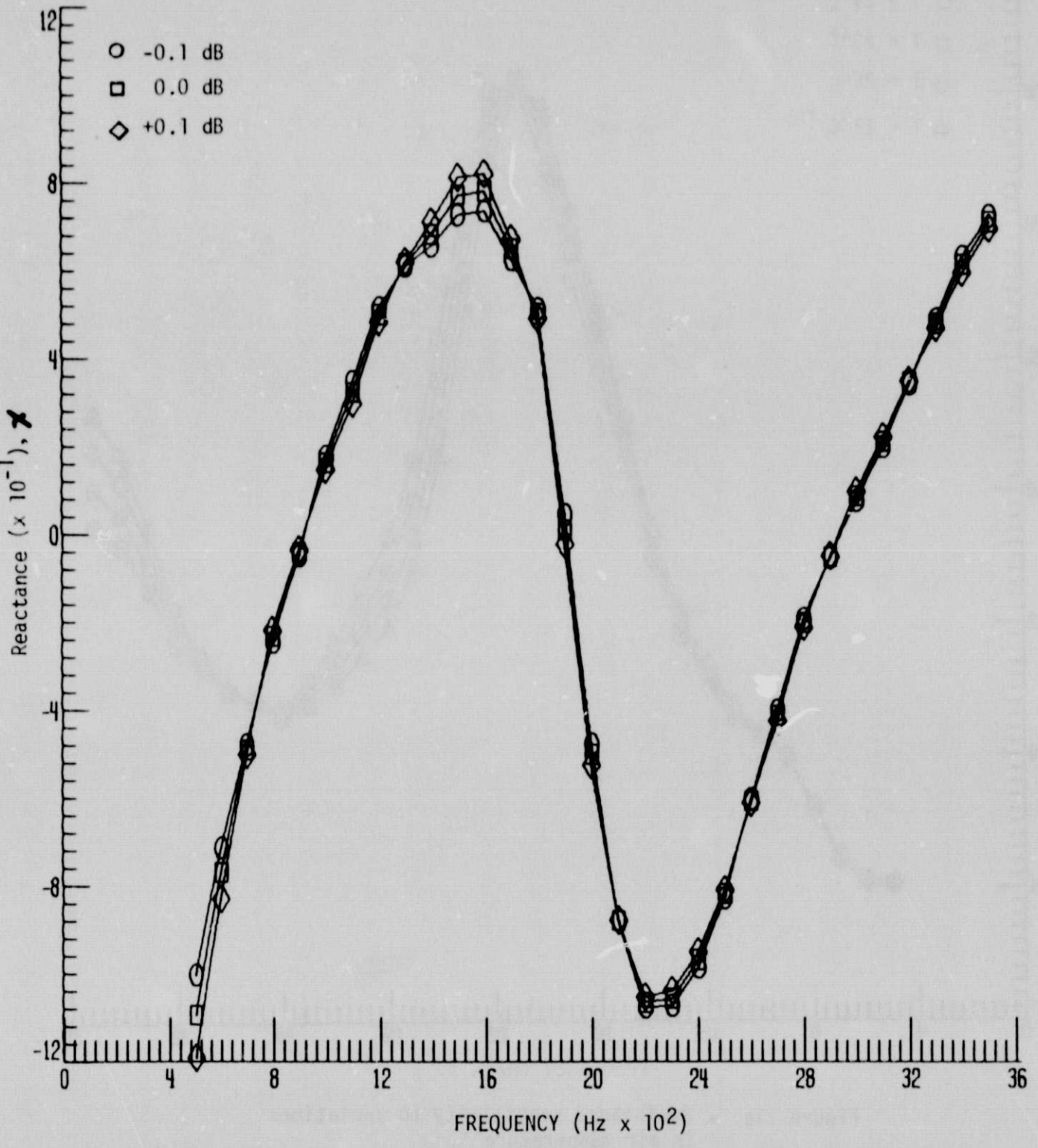

Figure 10b. - Reactance sensitivity to variations in pressure ratio.

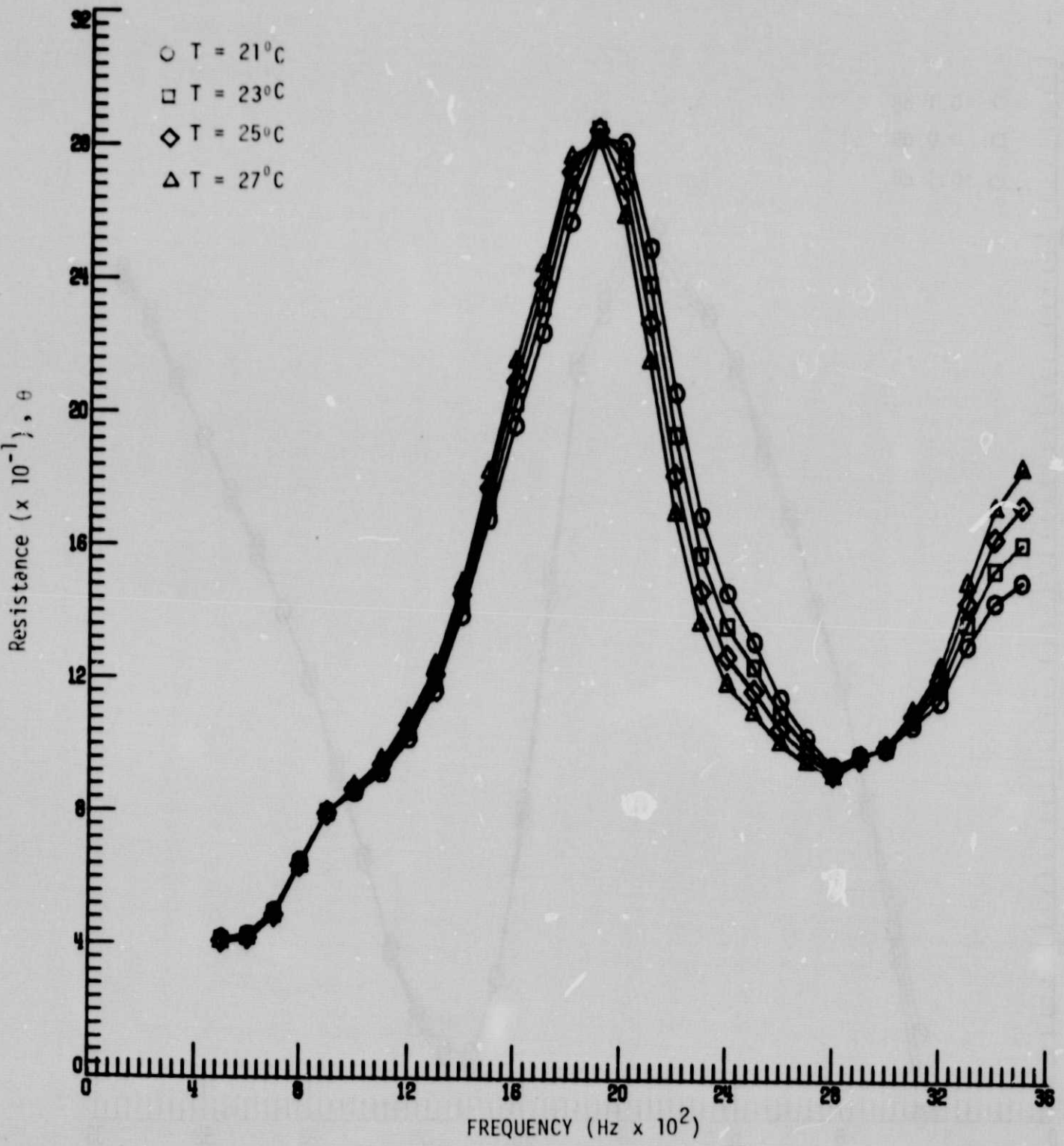

Figure 11a. - Resistance sensitivity to variations in air temperature T.

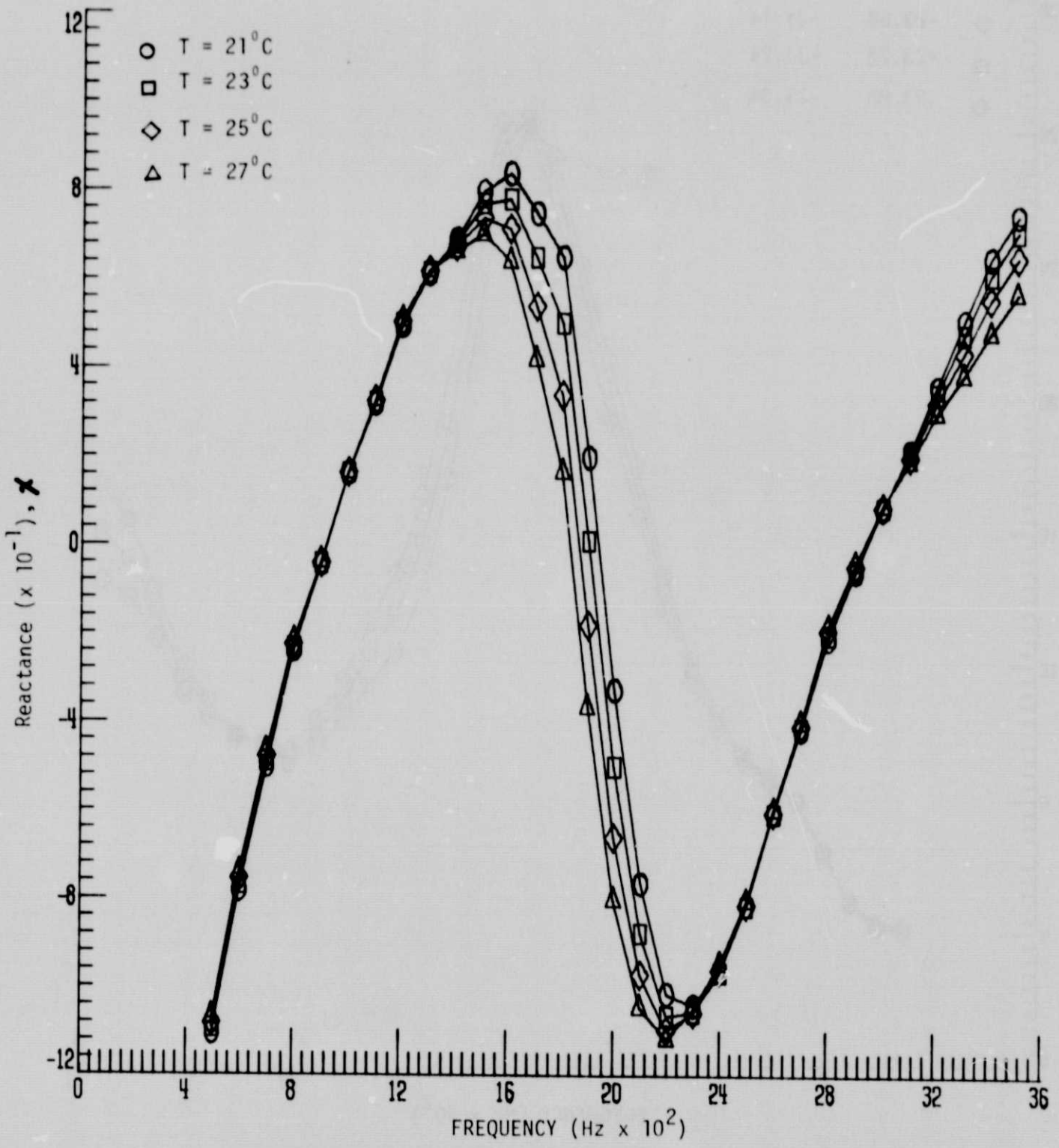

Figure 11b. - Reactance sensitivity to variations in air temperature T.

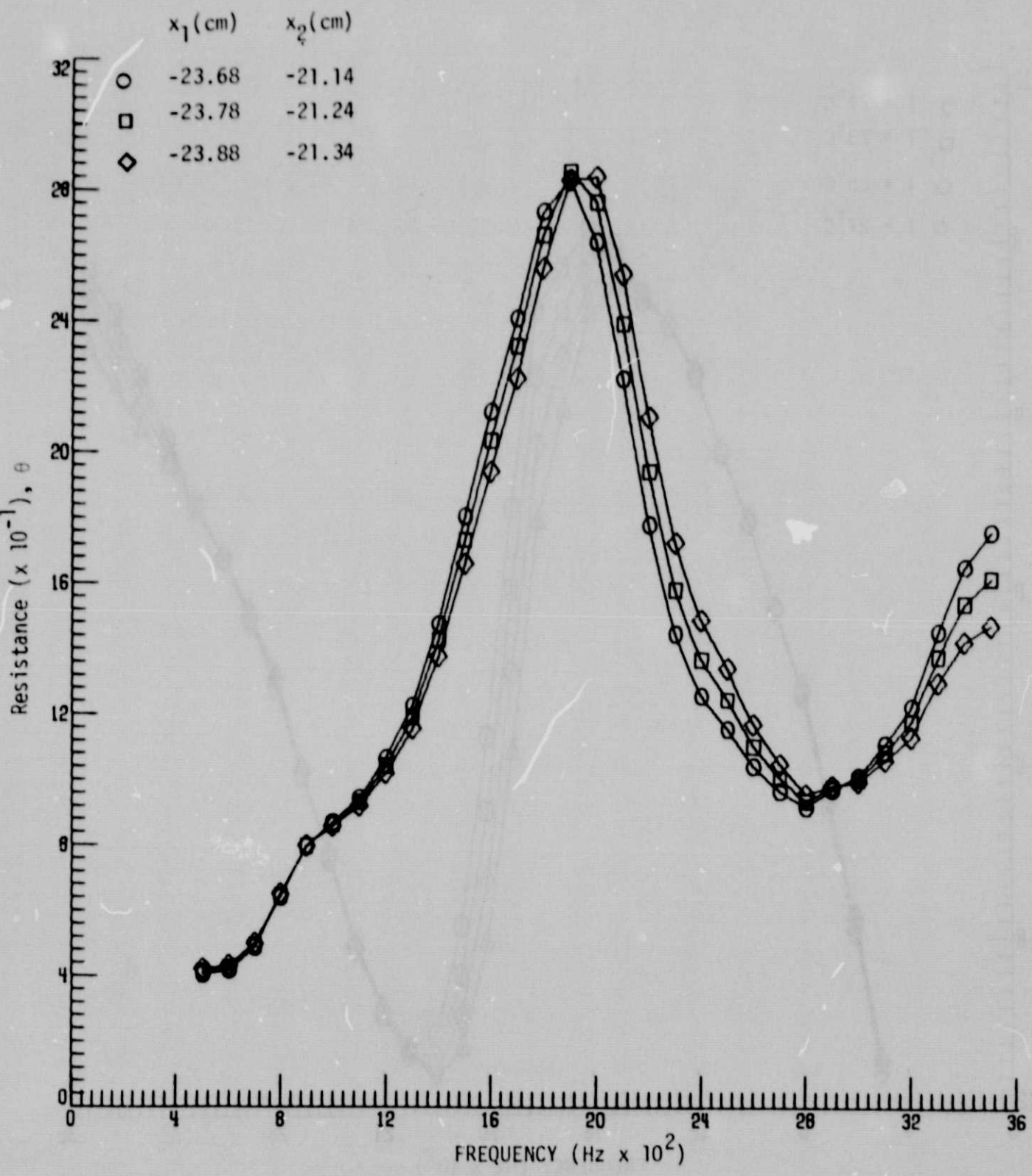

Figure 12a. - Resistance sensitivity to variations in microphone location with microphone spacing held constant (2.54 cm).

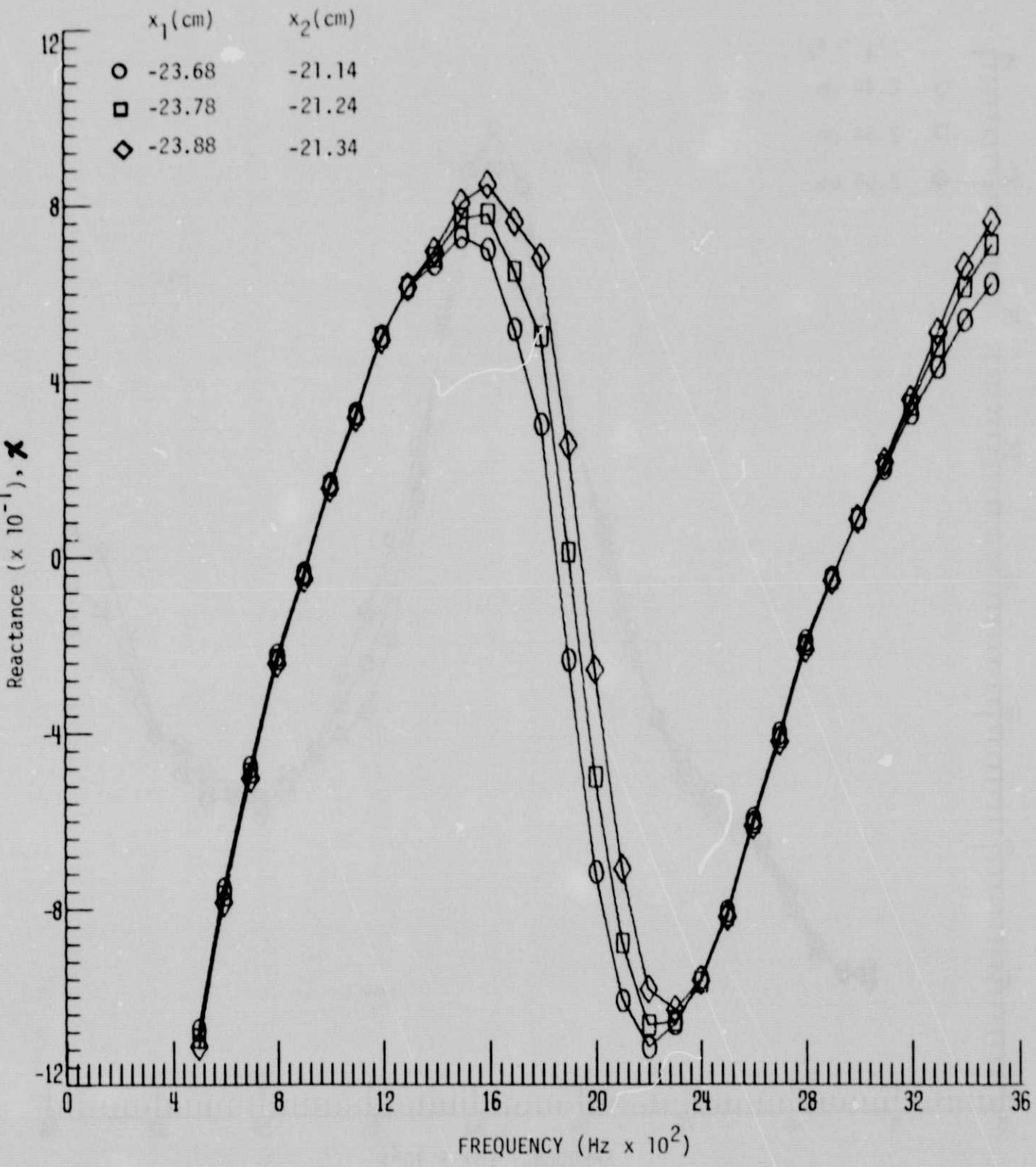

Figure 12b. - Reactance sensitivity to variations in microphone location with microphone spacing held constant (2.54 cm).

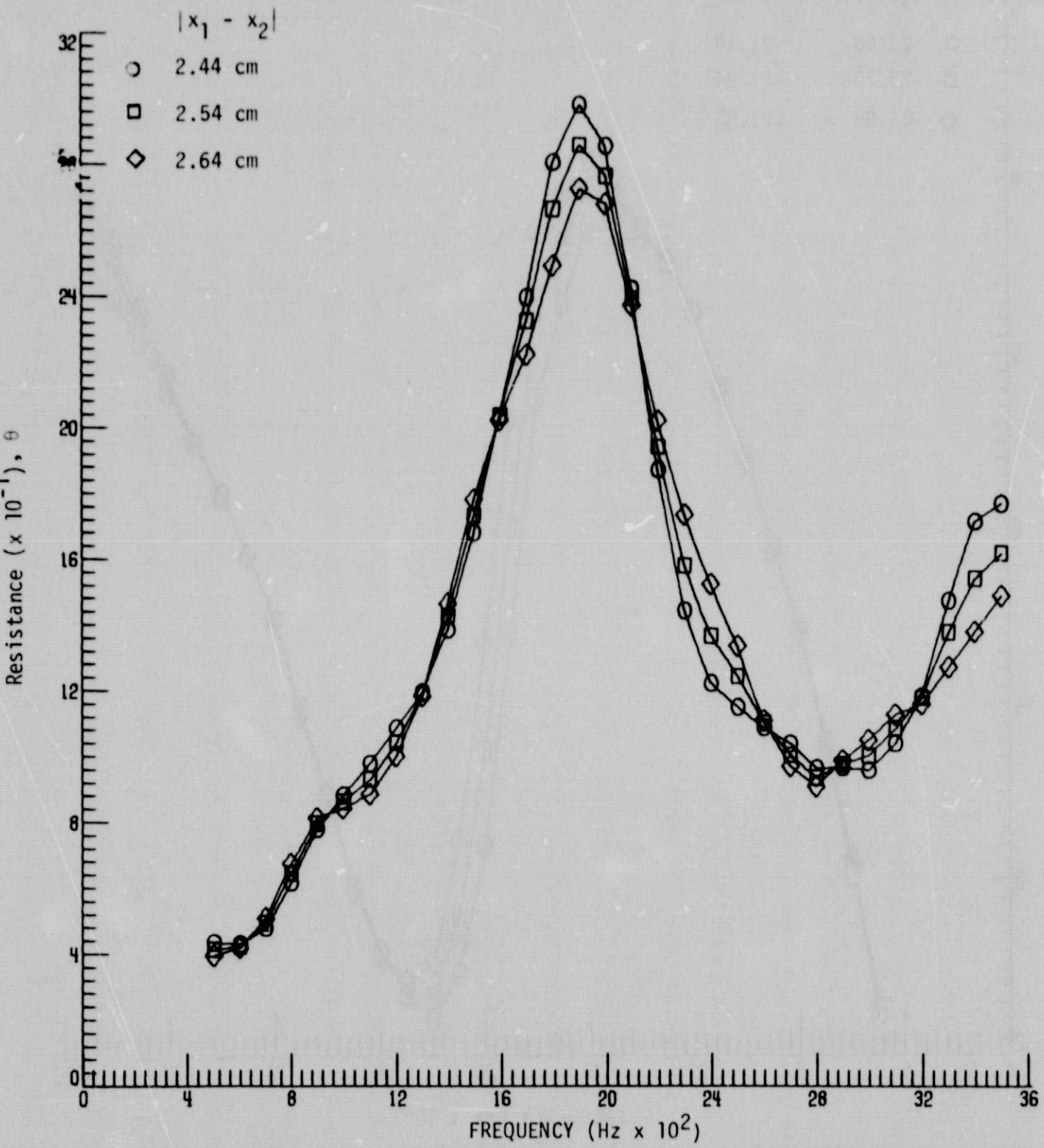

Figure 13a. - Resistance sensitivity to variations in microphone spacing with x_2 held constant.

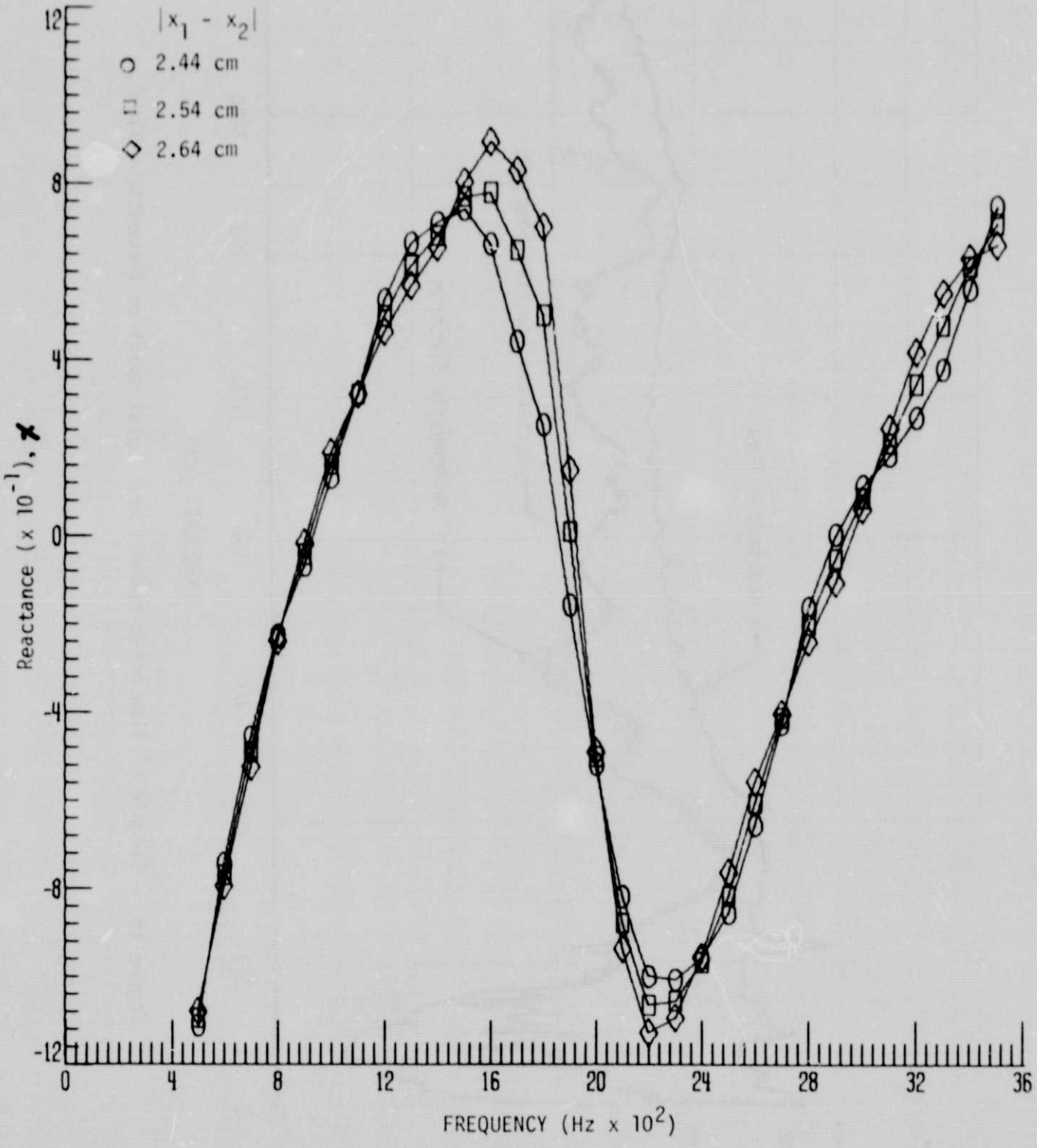

Figure 13b. - Reactance sensitivity to variations in microphone spacing with x_2 held constant.

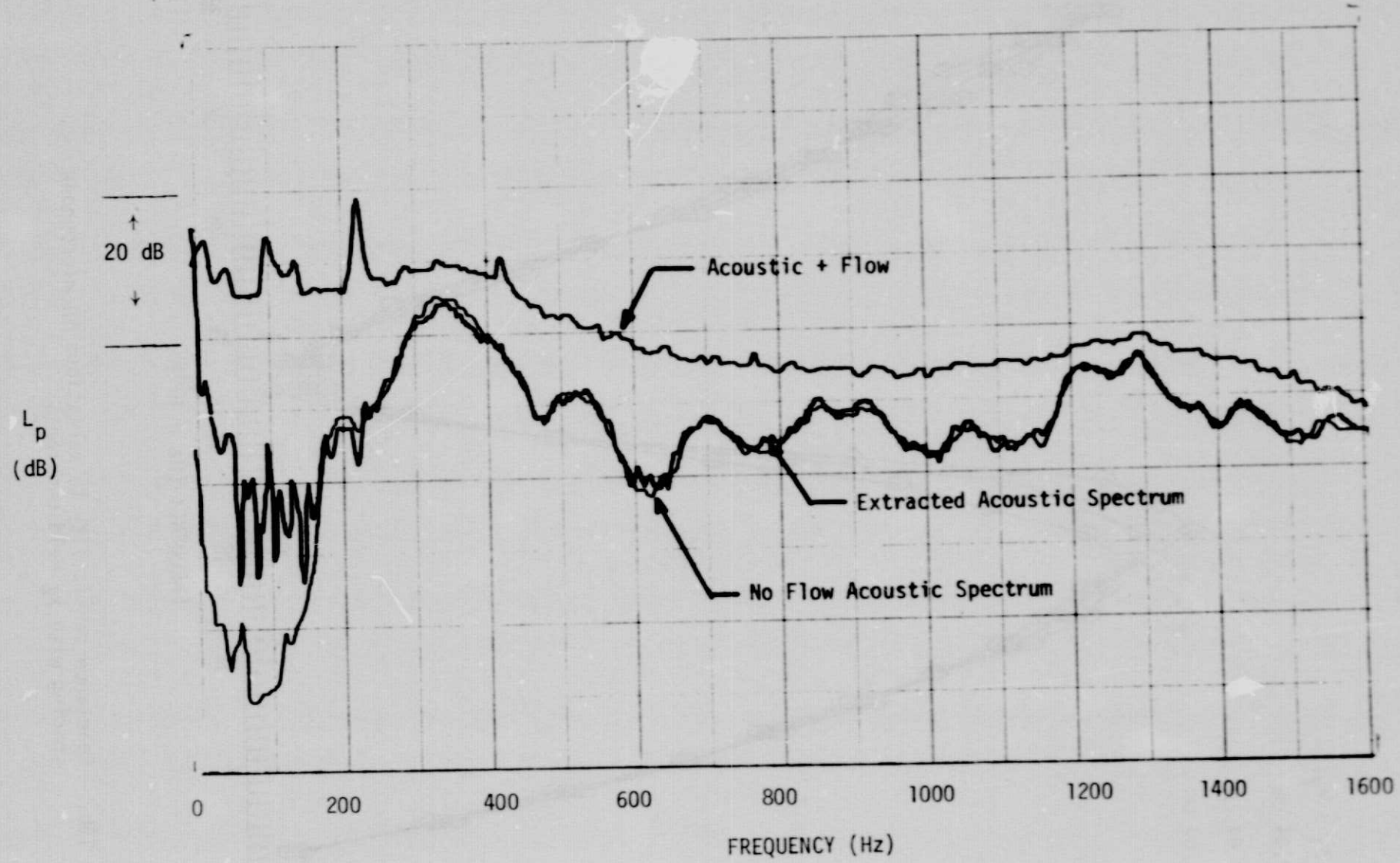

Figure 15. - Example of flow noise removal from total spectrum (acoustic + flow).